Ecological Engineering 62 (2014) 93–101

Contents lists available at ScienceDirect

Ecological Engineering

journal homepage: www.elsevier.com/locate/ecoleng

Investigating the spatial variability of dissolved organic matter quantity and composition in Lake Wuliangsuhai

Xu-jing Guo[a,*], Lian-sheng He[b,*], Qiang Li[c], Dong-hai Yuan[d], Yu Deng[a]

[a] Key Laboratory of Development and Application of Rural Renewable Energy, Ministry of Agriculture, Biogas Scientific Research Institute of the Ministry of Agriculture, Chengdu 610041, China
[b] Water Environment System Project Laboratory, Chinese Research Academy of Environmental Sciences, Beijing 100012, China
[c] School of Urban Economics and Public Administration, Capital University of Economics and Business, Beijing 100070, China
[d] Key Laboratory of Urban Stormwater System and Water Environment, Ministry of Education, Beijing University of Civil Engineering and Architecture, Beijing 100044, China

ARTICLE INFO

Article history:
Received 9 July 2013
Received in revised form 10 October 2013
Accepted 21 October 2013
Available online 17 November 2013

Keywords:
Dissolved organic matter
Excitation emission matrix (EEM) spectra
Fluorescent component
Parallel factor analysis
Principal component analysis

ABSTRACT

Dissolved organic matter (DOM) is an important component of the carbon cycle and a critical driver in controlling a variety of biogeochemical and ecological processes in aquatic environments. We reported the spatial variability of DOM quantity and composition which collected from Lake Wuliangsuhai in arid and semi-arid region. This study could serve as a useful tool to assess the dynamics of DOM in similar complex wetlands or lakes and provide a support for ecological environment governance and restoration. The results showed that five fluorescent components, including three humic-like (C1, C2 and C4), and two protein-like components (C3 and C5), can be identified by excitation emission matrix (EEM) spectra combined with parallel factor analysis (PARAFAC) in Lake Wuliangsuhai. The spatial variation of the components showed the difference in the dominant fluorescent component. There were dominant protein-like component C5 and humic-like component C2 in water and pore water. Components C3 and C4 were the main fluorescent components in 0–10 cm sediments. In 10–20 cm sediments, C1 and C3 were the dominant humic-like and protein-like component respectively. The PARAFAC–PCA displayed four PCA factors. The humic-like components C2 and C4 concurrently showed positive factor 1 loadings. Factor 2 was mainly explained by terrestrial and marine humic-like component C1. The autochthonous, tryptophan-like, fluorescent component C3, showed positive factor 3 loadings. The autochthonous, tyrosine-like, fluorescence component C5, having a low factor loading in other three factors, showed extremely high factor 4 loading. The EEM–PARAFAC combined with PCA showed varying contributions of terrestrial versus autochthonous DOM sources for the different regions in the wetland, suggesting that differences in human activities control DOM dynamics.

1. Introduction

Dissolved organic matter (DOM) is known to play many important roles in freshwater ecosystems, which influences water quality, the speciation and transport of metals, the distribution and bioavailability of hydrophobic contaminants, and the cycling of trace elements (Backhus et al., 2003; Holbrook et al., 2006; Yamashita and Jaffé, 2008). The changes in the structure, composition, and the relative abundance of DOM controlled many of these processes. The DOM can be mainly divided into two groups – natural organic matter (NOM) and anthropogenic organic matter (AOM, i.e., agricultural wastes, and industrial organic pollutants) (Wang et al., 2007). Rapid development of industry and agriculture has increased the amount of AOM entering the total DOM pool, which results in great differences in the structure, composition and the relative abundance of DOM. The reactivity and release of DOM from aquatic ecosystems to the atmosphere may vary depending on its overall composition (Benner and Kaiser, 2011). Due to the complexity and heterogeneity of DOM, tracing the difference in the composition of DOM with traditional chemical analysis is rather difficult. However, the changes in DOM fluorescence can reflect the variations in DOM composition from several autochthonous or allochthonous sources resulting from physical, biological, and chemical processes that occur in the water column (McKnight et al., 2001; Stedmon et al., 2007; Singh et al., 2010).

Fluorescence spectroscopy provides information about the composition and source of DOM, without requiring isolation or concentration prior to analysis, which has been widely used to characterize the DOM in aquatic environments (Stedmon and

* Corresponding authors. Tel.: +86 15198191696; fax: +86 28 85215106.
E-mail addresses: gxj530520@126.com (X.-j. Guo), heliansheng08@126.com (L.-s. He).

0925-8574/$ – see front matter © 2013 Elsevier B.V. All rights reserved.
http://dx.doi.org/10.1016/j.ecoleng.2013.10.032

Markager, 2005; Wei et al., 2009; Kowalczuk et al., 2010; Lai et al., 2013). Three-dimensional excitation–emission matrix (EEM) spectroscopy has also been used to distinguish different types and sources of DOM in natural waters, which can characterize the DOM and identify protein-like and humic-like fluorescence peaks in water samples from different aquatic environments (Coble, 1996). However, traditional peak picking techniques might not evaluate the exact changes in fluorescence intensity of protein-like and humic-like because of different fluorescence peaks overlap (Maie et al., 2007). Recently, statistical tools such as parallel factor analysis (PARAFAC) have been used to identify individual fluorescent components in a water sample (Stedmon et al., 2003; Kowalczuk et al., 2009; Hong et al., 2012).

PARAFAC analysis of EEM data has also been used to characterize the fluorophore DOM and trace photochemical and microbial reactions with organic matter (Stedmon and Markager, 2005; Stedmon and Bro, 2008), which can be applied to decompose fluorescence EEMs into different independent groups of fluorescent components and reduce the interference among fluorescent compounds (Andersen and Bro, 2003). The PARAFAC model provides a unique solution to the EEM dataset of DOM and is argued as a powerful tool for the assessment of DOM. Humic-like and protein-like substances are two primary fluorescing groups in the DOM. Humics are complex mixture of aromatic and aliphatic compounds derived from the decay of organic matter while protein-like substances are associated with high biological activity (Singh et al., 2010). PARAFAC modeling can efficiently identify these two classes of fluorophores from the DOM and determine the dominance of a particular class in an environment. Principal component analysis (PCA) of fluorescence EEMs was identified as a viable tool for monitoring the performance of pretreatment in membrane-based drinking water (Peiris et al., 2010; Peldszus et al., 2011). Moreover, to comprehensively assess the spatial differences and variability in the DOM, the PCA on the EEM–PARAFAC data set can also be used (Yao et al., 2011).

It has been widely reported on the biogeochemical cycling of DOM in the lakes. However, data are still scarce especially in arid and semi-arid region, and that serious soil erosion and salinization is spreading in that region. Further studies are still necessary for the sources and variability of DOM. Lake Wuliangsuhai (108°43′ ~ 108°57′ E, 40°27′ ~ 40°03′ N) is the biggest fresh water wetland in the Inner Mongolia, Yellow River basin. The soils around the Lake Wuliangsuhai region have suffered from serious erosion and salinization as reported by Yu et al. (2010). The wetland is filled by the drainage from surrounding agriculture and the upstream industrial wastewater and domestic sewage water. The former accounts for 96% of total volume of water in the wetland, and the rest contributes to only 4% of water. These effluents discharged into the Yellow River after being purified by Lake Wuliangsuhai. The wetland protects the ecological environment of the Yellow River. Meanwhile, these contaminants resulted in the difference in the structure and composition of DOM. The aims of this study were to (1) investigate the variability and differences of DOM from water, pore water and sediment in Lake Wuliangsuhai using the EEMs combined with PARAFAC modeling, and (2) characterize the sources, spatial differences and similarities of the components and abundance of DOM by EEM–PARAFAC and PCA.

2. Materials and methods

2.1. Sample collection and pretreatment

Seven typical representative water samples (W1–W7) were collected from Lake Wuliangsuhai with thoroughly rinsed 5 l pre-washed polyethylene bottles on November 18, 2009 (Fig. 1).

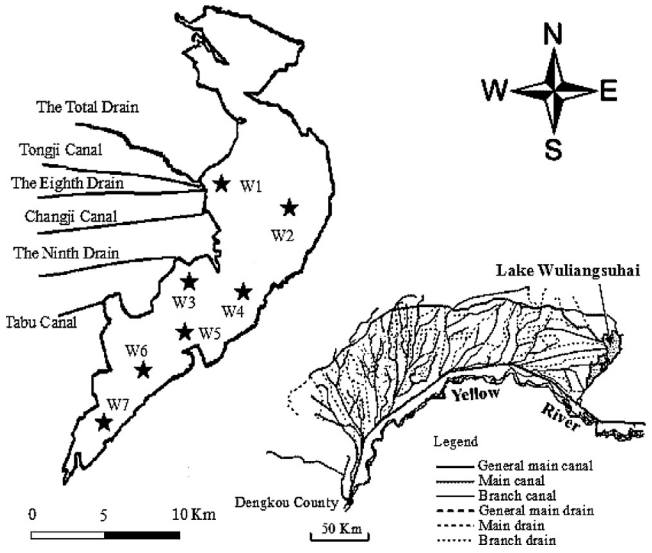

Fig. 1. Map of the Lake Wuliangsuhai shows (a) the locations of three canals and three drains, (b) agricultural irrigation and drainage network at the upstream area of Lake Wuliangsuhai and (c) seven sample sites: W1 (40°59′35.2″ N, 108°49′56.8″ E), W2 (40°59′49.2″ N, 108°56′28.0″ E), W3 (40°53′06.8″ N, 108°44′42.3″ E), W4 (40°53′23.64″ N, 108°52′19.59″ E), W5 (40°52′37.85″ N, 108°50′19.70″ E), W6 (40°51′28.68″ N, 108°47′34.08″ E) and W7 (40°46′49.0″ N, 108°42′14.6″ E).

W1 is located in the downstream areas of the Total Drain and received the upstream industrial wastewater and domestic sewage from the Total Drain. W2 is close to Nature Reserve. W3 is influenced by drainage of farmland irrigation from the Ninth Drain. W4, W5 and W6 are located in the eastern lake, where has no industry or dense residential area. W7 is located in the lake outlet area. Water samples were collected from the half of water depth. They were immediately placed into a foam insulation box with refrigerant and transferred to the laboratory. On return to the laboratory, they were filtered through Whatman GF/F filters (nominal pore size 0.45-μm), and then stored in the dark at 4 °C.

Seven core sediment samples were collected using a home-made gravity sampler, whose geographic coordinates were consistent with water samples. All samples were immediately placed into foam insulation boxes with refrigerant to preserve the samples and transferred to the laboratory on ice. Two profiles sediment samples (0–10 and 10–20 cm) which were named as DS and DN, respectively were used in our study. Sediments were freeze-dried using lyophilizer (FD-1A-50, Bilon, China) and ground, followed by passing 100 mesh sieve. DOM extractions of seven samples were conducted by mixing one part of solid sample with two parts of ultrapure water and continuously shaking it for 24 h. Extracts were centrifuged for 10 min at 7000 rpm at 4 °C and filtered through a 0.45-μm membrane. Duplicate extracts were carried in the same way. Then, twenty eight sediment DOM samples were used to the next fluorescence scan. The surface sediment sample (0–10 cm) was centrifuged at 10,000 rpm for 10 min, filtered through a 0.45-μm membrane filter. These extracts were sediment pore water (P1–P7) for our study.

All DOM samples do not exceed 24 h in the dark at 4 °C until they were analyzed. Dissolved organic carbon (DOC) concentrations were measured using a total organic carbon (TOC) analyzer (muti N/C 2100, Analytikjena, Germany). Duplicate measurements were made depending on the volume of sample available. The container used in the experiment was soaked in dilute HNO_3 overnight and washed with ultrapure water.

2.2. Spectral analysis

UV–vis absorbance spectra were collected using a double-beam spectrophotometer (UV-1700, Shimadzu, Japan) in a 1 cm quartz cuvette at room temperature (20 °C) over the wavelength range of 200–500 nm with ultrapure water as the reference. The apparatus was controlled by a computer using UVProbe software. DOC data were used to determine SUVA, which is an indicator of DOM aromaticity and defined as the UV absorption at 254 nm in inverse meters normalized to the DOC concentration in mg C/L (Weishaar et al., 2003).

All EEM fluorescence spectroscopy of DOM was measured using a Hitachi F-7000 fluorescence spectrometer (Hitachi, Japan) with a 150-W Xenon arc lamp as the light source. The scanning ranges were 200–450 nm for excitation, and 280–550 nm for emission. The slit widths were 5 nm for excitation and emission monochromators. Readings were collected at 5-nm intervals for both excitation and emission wavelengths, using a scanning speed of 1200 nm min^{-1}. The bandpass widths were 5 nm for both excitation and emission. Duplicate measurements were carried out depending on the volume of sample available. A fluorescence response to a blank solution (Milli-Q water) was subtracted from the spectra of each sample to eliminate the water Raman scatter peaks (McKnight et al., 2001; Chen et al., 2003). Each blank subtracted EEM was multiplied by the respective dilution factor and Raman-normalized by dividing by the integrated area under the Raman scatter peak of the corresponding Milli-Q water (Lawaetz and Stedmon, 2009) and the fluorescence intensities reported in Raman units (RU).

2.3. PARAFAC modeling

The EEM data obtained from the filtered and extracted DOM samples was modeled with PARAFAC, a decomposition method for reducing an EEM dataset into a set of trilinear terms and a residual array (Bro, 1997):

$$x_{ijk} = \sum_{f=1}^{F} a_{if} b_{jf} c_{kf} + \varepsilon_{ijk} i = 1, \ldots, I; \quad j = 1, \ldots, J; k = 1, \ldots, K \tag{1}$$

where F is the number of components (individual fluorophore moieties) and ε_{ijk} are the residual elements of the model; X_{ijk} is the fluorescence intensity of the ith sample at the kth excitation and jth emission wavelength; a_{if} is directly proportional to the concentration of the fth fluorophore in the ith sample (defined as scores); b_{jf} and c_{kf} are estimates of the emission and excitation spectra respectively for the fth fluorophore (defined as loadings), respectively (Stedmon et al., 2003). Finally, ε_{ijk} is the error term representing the variability not accounted for by the model. The principle behind the model is to minimize the sum of squared residual ε_{ijk}.

The EEM spectra samples were analyzed via PARAFAC. The analysis was carried out in Matlab 7.0 using the DOMFluor toolbox (Stedmon and Bro, 2008) and split-half analysis was further performed to validate the reliability of the model results (Stedmon et al., 2003). The utility of using PARAFAC with EEM data is that individual fluorophores moieties can be identified and their relative concentrations quantified in complex mixtures if the correct number of components are chosen and outliers are first identified and then removed from the dataset. F_{max} (R.U., i.e. Raman units) gives an estimate of the relative concentration of each component (Stedmon and Markager, 2005).

Table 1
Summary of DOC, pH, $SUVA_{254}$ and FI.

Sites	DOC (mg C/L)	pH	$SUVA_{254}$ (L/mg C m)	FI
W1	50.17	7.77	0.49	1.73
W2	62.48	8.79	0.58	1.61
W3	44.96	7.70	0.44	1.75
W4	58.29	7.94	0.78	1.59
W5	57.93	7.85	0.67	1.60
W6	59.16	8.09	0.73	1.59
W7	66.77	8.58	0.51	1.60
P1	173.60	7.96	0.12	1.82
P2	164.70	8.04	0.30	1.58
P3	231.30	8.19	0.13	1.63
P4	121.00	8.08	0.47	1.58
P5	116.10	8.09	0.38	1.62
P6	119.20	8.12	0.42	1.58
P7	98.91	8.40	0.37	1.57
DS1	81.38	8.14	0.67	1.71
DS2	91.50	8.00	0.75	1.59
DS3	49.10	8.47	0.63	1.51
DS4	81.63	8.26	1.22	1.55
DS5	128.50	8.23	1.27	1.72
DS6	42.38	8.40	1.33	1.48
DS7	85.13	8.65	0.87	1.75
DN1	33.27	8.21	4.17	1.71
DN2	63.78	8.05	1.50	1.53
DN3	22.62	8.71	3.51	1.59
DN4	54.72	8.34	2.80	1.56
DN5	28.74	8.17	2.87	1.56
DN6	12.96	8.42	2.91	1.57
DN7	42.57	8.59	4.60	1.68

2.4. Principal components analysis (PCA)

PCA was performed using the SPSS 16.0 statistical software. PCA is used to identify the principal components (PCs) that can be interpreted as 'type' spectra that permit the identification of compounds which comprise, and account for the bulk of the variation in the fluorescence spectra of DOM. The potential non-independence of the spectral data can affect the result of PCA. Therefore, KMO and Bartlett's test were used to test partial correlation and dependence. Meanwhile, all spectral data were rotated using the Varimax Raw algorithm to maximize the variance between spectra and maximize the loading on individual PCs in the data matrix.

3. Results and discussion

3.1. DOC, pH and optical properties

The DOC concentrations, pH and two spectral parameters for each site are summarized in Table 1. For poor irrigation and drainage management, increasing salts have accumulated in the wetland. Therefore serious salinization occurred around the wetland that resulted in all samples appeared an alkaline pH between 7.70 and 8.79. DOC ranged from 44.96 to 66.77 mg C/L in water samples, where site W3 showed a relatively low concentration of DOC. Fig. 1 showed that site W3 was located in the estuary of the Ninth Drain which transported the drainage of farmland irrigation into the wetland. However, due to the impact of serious soil erosion and salinization, the drainage of farmland irrigation appeared the high salt content and low DOC concentration (Guo et al., 2011). The sedimentation of particulate organic matter (POM) from surface waters toward the sediment and the export of DOM from the surface to deeper waters by mixing and downwelling of water parcels. Consequently, the pore water showed significantly high DOC concentration. Both POM and DOM are subject to microbial mineralization, and most of the organic carbon will be returned to dissolved inorganic carbon within a few decades (Jiao et al., 2010). The result is that DOC concentration decreased with increasing

depth in sediments, suggested a microbial degradation. However, an evidently high DOC concentration existed at site DS5 owing to the rotten reeds.

The SUVA values were observed to be significantly higher for DN sediment samples compared to all the other samples, suggesting significant contributions of highly aromatized DOM exported from the DN sediments. The increased contributions of microbial-derived DOM with pore water (and associated enhancements in DOM degradation) may result in a decrease in the aromaticity. The subsequent PARAFAC analysis will indicate the increased contributions of microbial-derived DOM in the pore water. Water samples also obtained relatively lower the SUVA values compared to sediment samples, indicating a low aromaticity resulting from the water inflow of high salt content, especially in the site W3.

The Fluorescence index (FI) was determined as the ratio of the emission intensity at a wavelength of 450 nm to that at 500 nm, obtained at an excitation of 370 nm (McKnight et al., 2001). A value of 1.4 indicates that the DOM is terrestrial in nature while a value closer to 1.9 is an indicator that the source of aquatic DOM is microbial (McKnight et al., 2001). FI values ranged from 1.48 to 1.82 throughout all samples, with the highest value observed in site P1, while the DS6 site had the lowest value. Due to the impact of industrial wastewater and domestic sewage from the Total Drain, W1, P1, DS1 and DN1 obtained a significantly high FI value, suggested high microbial sources of DOM. Hood et al. (2003) suggested a high FI value around 1.74 resulting from microbial sources of DOM dominate. FI values reflected the contributions of terrestrial versus autochthonous DOM sources in Lake Wuliangsuhai.

3.2. Fluorescent components of DOM

The spectral characteristics of the modeled PARAFAC components are presented in Fig. 2. Five separate fluorescent components were identified for DOM spectra from the PARAFAC model. Fig. 2 explains the excitation and emission loadings identified in the five component PARAFAC model. All components have two peaks, except for component 1. In general, the components have single emission maxima with two excitation maxima. Component 1 (C1) is centered at a maximum excitation/emission (Ex/Em) wavelength pair of 305/425 nm and relates to the marine humic-like fluorescence peak M (Murphy et al., 2008; Yamashita et al., 2008; Baghoth et al., 2011) that is defined as a mixture of dissolved and colloidal substances produced in situ as a byproduct of microbial respiration (Parlanti et al., 2000) and has been proposed to be produced by the degradation of the DOM by heterotrophic microbes (Pautler et al., 2012). However, traditional EEMs did not detect the component (Guo et al., 2011, 2012a) (Fig. 3).

Component 2 (C2) had a primary fluorescence peak at an Ex/Em wavelength pair of 230 nm/408 nm and a secondary peak at 305 nm/408 nm, which also relates to marine and terrestrial humic substances whose main constituent is fulvic-like acid (Holbrook et al., 2006; Stedmon et al., 2007; Kowalczuk et al., 2009). This component was categorized as the traditional terrestrial humic-like peaks A. The spectral features were also similar to those reported for terrestrial-derived humic-like PARAFAC components (Murphy et al., 2008; Yamashita et al., 2008). Studies suggested that the C2 is similar to those with terrestrial and marine precursors (Zhang et al., 2009; Osburn and Stedmon, 2011).

Component 3 (C3) was composed of two excitation maxima at 230 and 275 nm, with one emission peak centered at 345 nm, which was a typical protein-like substance, such as an autochthonous tryptophan-like fluorescence that has been observed as an autochthonous tryptophan-like fluorescence peak T in both marine and terrestrial waters (Coble, 1996; Murphy et al., 2008; Fellman et al., 2010).

Component 4 (C4), at 260/460 nm and 360/460 nm respectively, is thought to represent humic material exported from terrestrial sources that were similar to the traditional terrestrial humic-like fluorescence peak C (Coble, 1996). C4 has been identified in DOM from a wide variety of aquatic systems, including those dominated by terrestrial and microbial inputs (Stedmon and Markager, 2005; Cory and McKnight, 2005; Ohno and Bro, 2006; Guéguen et al., 2011). Organic substances with fluorescence signals at short wavelength are associated with the presence of simple structural components with a low aromaticity, whereas fluorescence signals at long wavelength are related to the presence of complex structural components with a high conjugation degree (Senesi et al., 2003; He et al., 2011). Therefore, compared with C2, C4 has a red shift, indicating a higher degree of aromatic polycondensation and greater chemical stability.

Component 5 (C5) was protein-like component with tyrosine-like material, possessing a primary (secondary) excitation/emission wavelength pair of 230 (275)/308 nm. These fluorescence characteristics were categorized as the previously defined autochthonous tyrosine-like fluorescence peak B. This component was also similar to autochthonous protein-like PARAFAC components (Murphy et al., 2008; Yamashita et al., 2008).

3.3. Spatial variability of PARAFAC component scores

Fig. 4a shows that the C5 is the main protein-like component with tyrosine-like material. Site W1 has a very high relative abundance of C5, which accounting for a total concentration of 55.76%. Meanwhile, the C3 also showed a higher relative abundance in sight W1 relative to the other sites. Site W1 is located in the downstream areas of the Total Drain and received the upstream industrial wastewater and domestic sewage from the Total Drain. These pollutants made an increasing fluorescent protein-like substances which induced by microbial activity. Due to the impact of pollutants from the Total Drain, C3 and C5 showed relatively high abundance at site W2, 15.46% and 20.68% respectively. The relative abundance of C3 and C5 were the lowest at site W3 in comparison with the other six sites. They were 10.63% and 11.69% for C3 and C5 respectively. Site W3 was influenced by the drainage of farmland irrigation from the Ninth Drain, which has the high salt content and low microbial activity, and resulted in the lowest fluorescent protein-like components (Guo et al., 2012b).

The C2 occupied the dominant humic-like substances at seven sites, which have a relatively higher abundance than those of components C1 and C4. However, the relative abundance of humic-like substances in site W1 was obviously lower than those of other six sites. The results suggested that the pollution of industrial wastewater and domestic sewage has affected the distribution of fluorescent humic-like substances. Previous research showed a low fluorescence intensity of humic-like materials at site W3 (Guo et al., 2011). However, due to the impact of drainage of farmland irrigation, the high salt content and low microbial activity, humic-like substances became the dominant fluorescent component. Therefore, there were a high relative abundance of C2 and C4 at site W3. Furthermore, reeds acted as a natural filter, which resulted in the high relative abundance of C2 and C4 at sites W4, W5, W6 and W7.

In pore water DOM, the C2 was a more dominant fluorescent component (Fig. 4b). Site P3 obtained the highest relative abundance of the C2. In addition to site P7, the relative abundance of C1 has a slight increase in comparison with water DOM. The C5 was still the main protein-like component. However, site P7 has the highest relative abundance of C5 (31.41%). There was an obvious decrease in the relative abundance of C5 (30.45%) at site P1compared to site W1. Moreover, the relative abundance of the

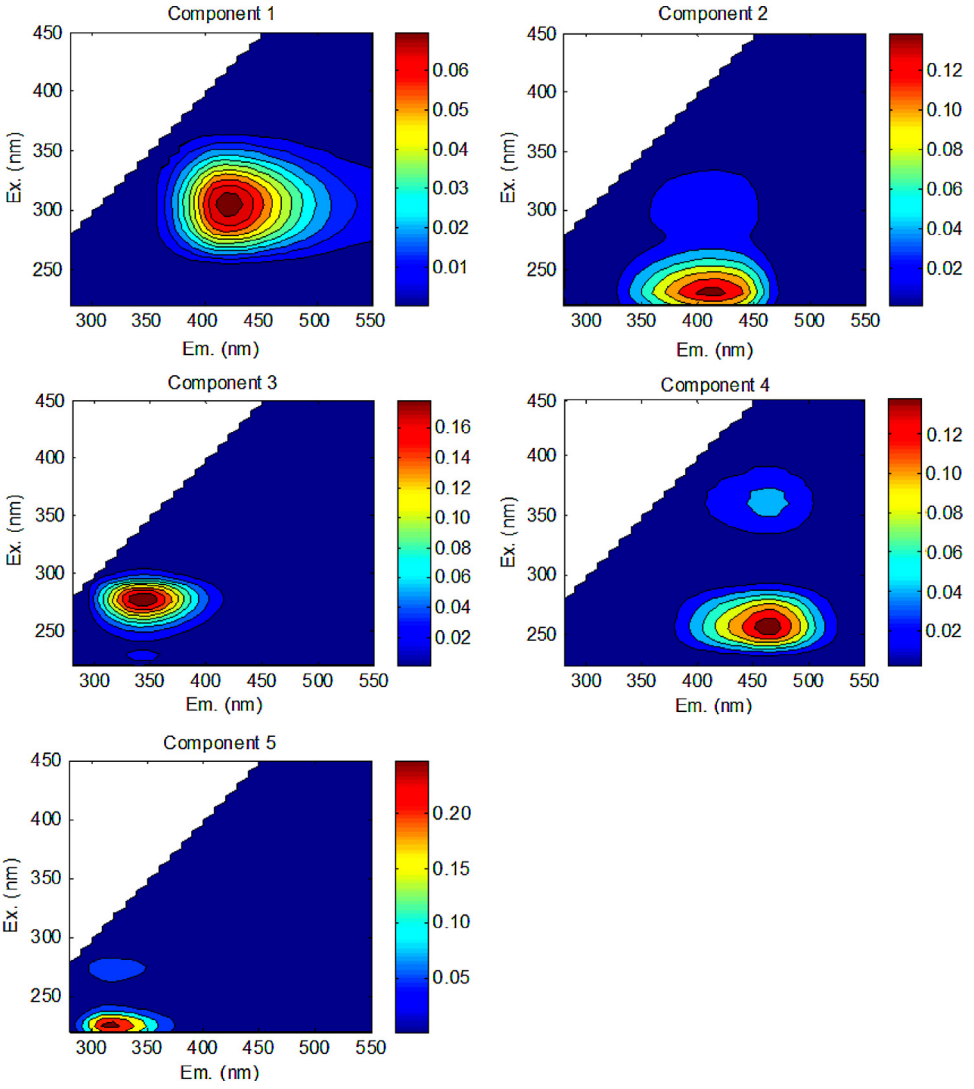

Fig. 2. Fluorescent components of DOM from Lake Wuliangsuhai identified by the PARAFAC model.

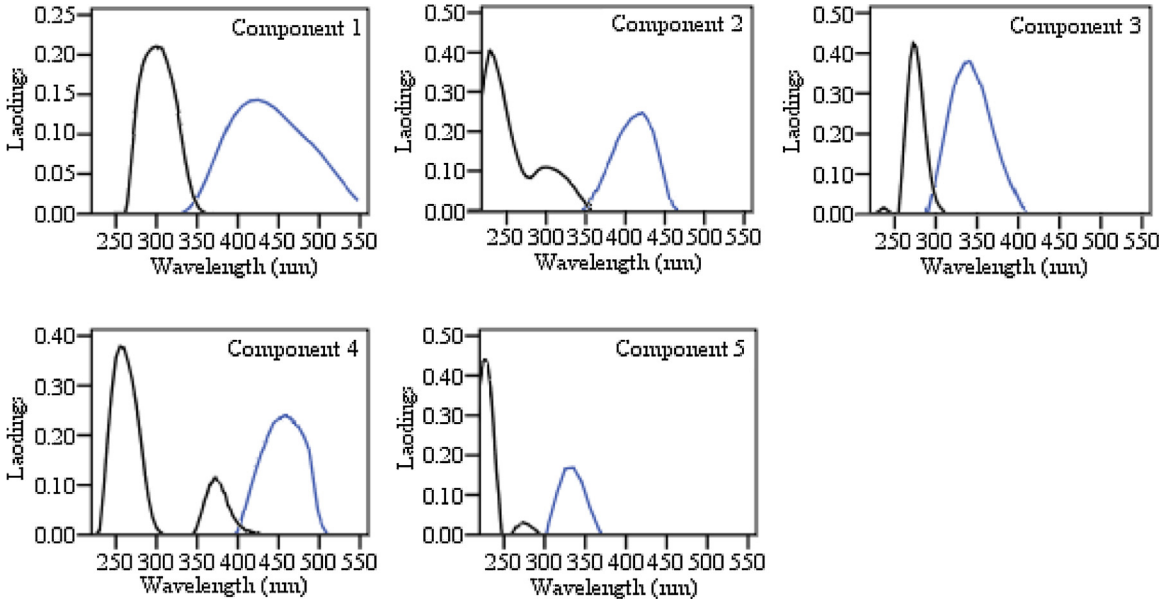

Fig. 3. Excitation (black lines) and emission loadings (blue lines) of the five components identified by the DOMFluor-PARAFAC model. (For interpretation of the references to color in the artwork, the reader is referred to the web version of the article.)

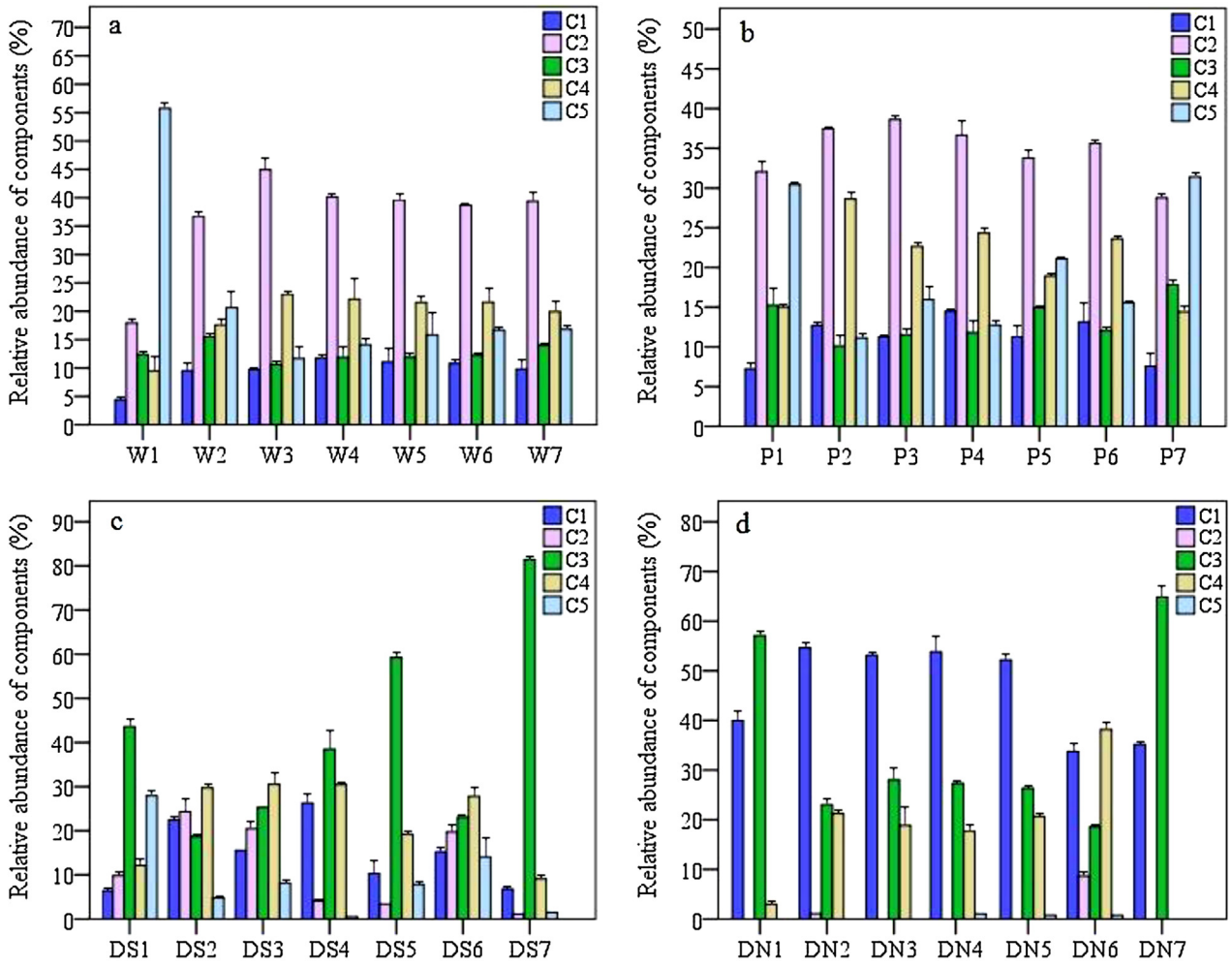

Fig. 4. The relative abundance of five fluorescent components in four types of samples. W, P, DS and DN represent water, pore water, sediment (0–10 cm) and sediment (10–20 cm) samples.

C3 had an obvious increase at sites P1, P5 and P7 than those at W1, W5 and W7.

There was a major change in the distribution of fluorescent component that C3 became a dominant protein-like fluorescent component (Fig. 4c). These results suggested that the protein-like fluorescence from autochthonous microbial activity shifted from shorter wavelength to longer wavelength. Especially in site DS7, C3 obtained the extremely high relative abundance (81.44%). There was a possible reason that the accumulation of pollutants from the upstream sewage and the Yellow River's backward flow provided the carbon source for the activity of microorganisms. It can also be seen from Fig. 4c that sites DS4 and DS7 presented a significantly low the relative abundance of C5, 0.57% and 1.50% respectively.

Fig. 4c showed that the dominant humic substance showed a transition from fulvic-like acid (C2) to humic-like acid (C4). The fluorescence signals of organic substances at short wavelengths are related to simple structural components with a low degree of aromatic polycondensation, whereas fluorescence signals at long wavelengths are associated with complex structural components with a high degree of conjugation. Organic substances with a higher degree of aromatic polycondensation generally have higher chemical stability, increasing the residence time of organic matter in the environment (Santos et al., 2010). Therefore, DOM indicated a higher degree of aromatic polycondensation and chemical stability in 0–10 cm sediment than those in water and pore water. Compared to sites P2 and P4, the relative abundance of the C1 has an obvious increase in sites DS2 and DS4.

Fig. 4d showed that C1 has a significant increase in 10–20 cm sediment which was the main humic-like fluorescent component. The dominant C3 obtained an extremely high the relative abundance in sites DN1 and DN7 (57.09% and 64.85% respectively) than those in the other sites. Site DN6 was the only one site which can find all five components. Although C5 was present in sites DN4, DN5 and DN6, their relative abundance was very low. C2 can be found in sites DN2 and DN6. However, the relative abundance of C2 appeared extremely low (1.09%) in site DN2.

Overall, fluorescent components identified by PARAFAC model in Lake Wuliangsuhai showed a spatial variability. Different sources and pollution situation were the main factors to cause such a difference. The combination of EEMs and PARAFAC is a powerful tool in the assessment of DOM in the wetland ecosystems.

3.4. Principal component analysis of PARAFAC component distributions

To further assess the changes in fluorescent components, PCA was performed for the EEM–PARAFAC data set, by using the relative concentration of the five PARAFAC components. The communality

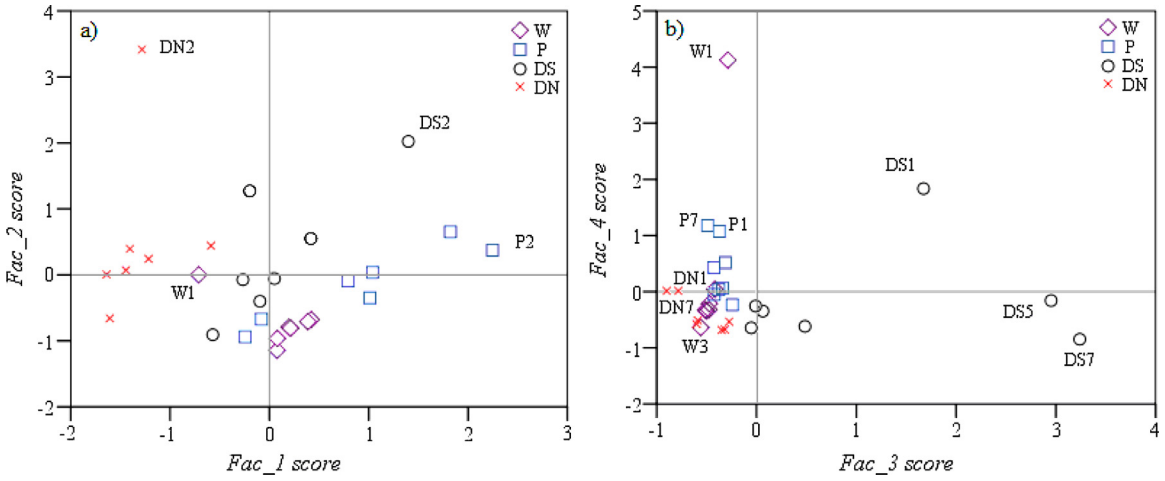

Fig. 5. Property–property plots of PCA factor scores of all samples.

extracted from five components ranges from 0.961 to 0.999, indicates that more information was retained when variances convert to factor space. Two parameters, Kaiser-Meyer-Olkin (KMO) measure and Bartlett's test of sphericity (P) can be used to test the feasibility of PCA. PCA shows a smaller partial correlation between variables (KMO = 0.865) and a high dependence ($P < 0.001$). In general, the *KMO* value is higher than 0.5 and the P value is lower than 0.05 can be viewed as suitable for PCA. The PCA of all components yielded 4 PCs that account for 97.96% of the variance.

For all fluorescent PARAFAC components, the first and second axes of the PCA (factors 1 and 2) accounted for 31.09% and 23.34%, respectively, of the variance in fluorescent component. Similarly, the third and fourth axes of the PCA (factors 3 and 4) accounted for 22.74% and 20.79%, respectively. Each PCA factor is a linear combination of the five fluorescent components where the measured factors are dimensionless and can be either positive or negative:

$$\text{Factor1} = 0.074C1 + 0.874C2 - 0.037C3 + 0.871C4 + 0.157C5 \quad (2)$$

$$\text{Factor2} = 0.974C1 - 0.196C2 + 0.032C3 + 0.387C4 - 0.172C5 \quad (3)$$

$$\text{Factor3} = 0.030C1 - 0.314C2 + 0.993C3 + 0.225C4 + 0.036C5 \quad (4)$$

$$\text{Factor4} = -0.183C1 + 0.245C2 + 0.036C3 + 0.030C4 + 0.971C5 \quad (5)$$

The humic-like fluorescent components 2 and 4 concurrently showed positive factor 1 loadings. The two humic-like components had a high factor loading, indicated that there were dominated humic substances for the factor 1. Factor 2 was mainly explained by terrestrial and marine humic-like component C1, which showed positive factor 2 loadings. The autochthonous, tryptophan-like, fluorescent component C3, showed positive factor 3 loadings. The autochthonous, tyrosine-like, fluorescence component 5, having a low factor loading in other three factors, showed extremely high factor 4 loading. Hence, the PARAFAC–PCA in this study could separate the characteristics of the DOM fluorescent components, namely the source strength of the humic-like components versus the contributions of protein-like components in the total fluorescence analyses (Yamashita et al., 2010; Yao et al., 2011).

The PCA factor scores of all samples are plotted in. The figure shows a marked difference in different samples. Most samples were more relatively scattered in Fig. 5a. However, water samples were more clustered except site W1. Site W1 obtained a very low factor 2 score, indicated a low relative concentration of fluorescent component C1 (4.42%). Similarly, sediment samples (10–20 cm) were more clustered except site DN2. Site DN2 showed an extremely high factor 2 score, which also indicated a high relative concentration of terrestrial and marine humic-like component C1 (54.63%). Furthermore, in 0–10 cm sediment samples, DS2 demonstrated the highest first and second PCA scores (1.398 and 2.025, respectively), suggested a higher humic-like fluorescent components (including C1, C2 and C4, a total relative abundance of 76.54%). Sample P2 was located in the region with higher first and lower second PCA score compared to the other pore water samples, which indicated a high total relative abundance of C2 and C4 (66.07%).

However, Fig. 5b showed that most samples were more relatively clustered. Four samples including a water sample (W1) and three 0–10 cm sediment samples (DS1, DS5 and DS7) showed an obvious difference compared to the other samples. W1 obtained the highest factor 4 score, showing that component C5 was the dominated protein-like fluorescent component. The result was consistent with the PARAFAC in Fig. 4. Similarly, DS1, DS5 and DS7 samples showed higher factor 3 score, which had the dominated component C3. Moreover, DS1 sample also obtained a relatively high factor 4 score, suggested a higher relative abundance of component C5 than those in other 0–10 cm sediment samples. In pore water samples, P1 and P7 showed relatively high factor 4 score, suggesting high microbial sources of DOM. It was consistent with the results of FI values that relatively high microbial sources of DOM were observed at sites DN1 and DN7. However, FI value suggested a high autochthonous DOM at site W3, but the results of PCA have not shown obviously high factor 3 score or factor 4 score. The increasing salt content from the agricultural water discharge was a possible reason for the changes in fluorescent component.

3.5. Analyzing the sources of DOM using the EEM–PARAFAC combined with PCA

The PCA in conjunction with EEM–PARAFAC is a powerful tool in analyzing the relative abundance of PARAFAC components. The

separation of samples along the PCA axes can explain clearly the variability in DOM between water and sediment samples. Moreover, PCA of the relative abundance of PARAFAC components can also identify sources of DOM and water pollution (Yao et al., 2011). The PCA results suggest that there are both terrestrial and autochthonous DOM inputs from drainage channels to Lake Wuliangsuhai, including humic-like and protein-like components. Agricultural return water, industrial wastewater and domestic sewage of terrestrial humic-like components play an important role in the wetland DOM. The fulvic-like component, C2, was a dominant component in water and pore water (Fig. 4). This dominance corresponds to the impact of terrestrial humic-like components. The PCA results also showed a higher relative abundance of humic-like component C1 in 10–20 cm sediments compared to other types (Fig. 4). This type of fluorescence was originally thought to only persist in productive oceanic environments but now has also been observed in freshwaters impacted by agriculture (Stedmon and Markager, 2005; Coble, 2007; Jørgensen et al., 2011).

The main contribution of autochthonous tryptophan-like components C5 to wetland samples is due to the autochthonous production of DOM in the wetland ecosystems. Due to the increasing terrestrial pollutant inputs, frequently microbial activity has more significantly affect the DOM in water and pore water than those in sediments. Specifically, W1 samples showed the highest factor 4 score, which highlighted the effect of industrial wastewater and domestic sewage in DOM quality.

The PCA results suggest that the tyrosine-like component, C3, was a dominant component in sediments. In addition to terrestrial pollutant inputs, the rotten reeds were a good carbon sources for microbial activity. Although far away from pollution sources, sites DS4 and DS5 also showed a high relative abundance of C3. In the wetland outlet area, water intrusion from the Yellow River carried a number of pollutants into the wetland. By sedimentation, those pollutants provided abundant nutrient for microorganisms and resulted in an autochthonous tyrosine-like fluorescence.

The EEM–PARAFAC combined with PCA showed varying contributions of terrestrial versus autochthonous DOM sources for the different regions in the wetland, suggesting that differences in human activities control DOM dynamics.

4. Conclusions

The PARAFAC and PCA techniques applied to fluorescence spectroscopy to study the DOM in Lake Wuliangsuhai presented unique results that the dominant protein-like and humic-like fluorescent components showed a transition in different source samples. Further, this study enabled us to quantify the compositional contributions by different fluorescent components in the wetland. The relative abundance of the identified components showed their distribution by allochthonous and autochthonous dissolved organic material in different sampling sites. This study supported the use of excitation emission matrix fluorescence in combination with parallel factor analysis and PCA to distinguish between different sources of dissolved organic matter. Its applicability could serve as a useful tool to assess the dynamics of DOM in similar complex wetlands or lakes and provide a support for ecological environment governance and restoration.

Acknowledgements

This work was financially supported by the 12th Five-Year National Science and Technology Support Plan (No. 2011BAD15B04), the National Natural Science Foundation of China (No. 51209003) and Science and Technology Development Plan of Jilin Province (No. 20110263).

References

Andersen, C.M., Bro, R., 2003. Practical aspects of PARAFAC modeling of fluorescence excitation–emission data. J. Chemometr. 17, 200–215.
Backhus, D.A., Golini, C., Castellanos, E., 2003. Evaluation of fluorescence quenching for assessing the importance of interactions between nonpolar organic pollutants and dissolved organic matter. Environ. Sci. Technol. 37, 4717–4723.
Baghoth, S.A., Sharma, S.K., Amy, G.L., 2011. Tracking natural organic matter (NOM) in a drinking water treatment plant using fluorescence excitationeemission matrices and PARAFAC. Water Res. 45, 797–809.
Benner, R., Kaiser, K., 2011. Biological and photochemical transformations of amino acids and lignin phenols in riverine dissolved organic matter. Biogeochemistry 102, 209–222.
Bro, R., 1997. PARAFAC: tutorial and applications. Chemometr. Intell. Lab. 38, 149–171.
Chen, W., Westerhoff, P., Leenheer, J.A., Booksh, K., 2003. Fluorescence excitation–emission matrix regional integration to quantify spectra for dissolved organic matter. Environ. Sci. Technol. 37, 5701–5710.
Coble, P.G., 1996. Characterization of marine and terrestrial DOM in seawater using excitation–emission matrix spectroscopy. Mar. Chem. 51, 325–346.
Coble, P.G., 2007. Marine optical biogeochemistry: the chemistry of ocean color. Chem. Rev. 107, 402–418.
Cory, R.M., McKnight, D.M., 2005. Fluorescence spectroscopy reveals ubiquitous presence of oxidized and reduced quinones in dissolved organic matter. Environ. Sci. Technol. 39, 8142–8149.
Fellman, J.B., Spencer, R.G.M., Hernes, P.J., Edwards, R.T., D'Amore, D.V., Hood, E., 2010. The impacts of glacier runoff on the biodegradability and biochemical composition of terrigenous dissolved organic matter in near-shore marine ecosystems. Mar. Chem. 121, 112–122.
Guéguen, C., Granskog, M.A., McCullough, G., Barber, D.G., 2011. Characterisation of colored dissolved organic matter in Hudson Bay and Hudson Strait using parallel factor analysis. J. Marine Syst. 88, 423–433.
Guo, X., Yuan, D., Li, Q., Jiang, J., Chen, F., Zhang, H., 2012a. Spectroscopic techniques for quantitative characterization of Cu (II) and Hg (II) complexation by dissolved organic matter from lake sediment in arid and semi-arid region. Ecotoxicol. Envion. Saf. 85, 144–150.
Guo, X., Jiang, J., Xi, B., He, X., Zhang, H., Deng, Y., 2012b. Study on the spectral and Cu (II) binding characteristics of DOM leached from soils and lake sediments in the Hetao region. Environ. Sci. Pollut. Res. 19, 2079–2087.
Guo, X.J., Xi, B.D., Yu, H.B., Ma, W.C., He, X.S., 2011. The structure and origin of dissolved organic matter studied by UV–vis spectroscopy and fluorescence spectroscopy in Lake in Arid and Semi-Arid Region. Water Sci. Technol. 63, 1010–1017.
He, X.S., Xi, B.D., Wei, Z.M., Guo, X.J., Li, M.X., An, D., Liu, H.L., 2011. Spectroscopic characterization of water extractable organic matter during composting of municipal solid waste. Chemosphere 82, 541–548.
Holbrook, R.D., Yen, J.H., Grizzard, T.J., 2006. Characterizing natural organic material from the Occoquan Watershed (Northern Virginia, U.S.) using fluorescence spectroscopy and PARAFAC. Sci. Total Environ. 361, 249–266.
Hong, H., Yang, L., Guo, W., Wang, F., Yu, X., 2012. Characterization of dissolved organic matter under contrasting hydrologic regimes in a subtropical watershed using PARAFAC model. Biogeochemistry 109, 163–174.
Hood, E., McKnight, D.M., Williams, M.W., 2003. Sources and chemical character of dissolved organic carbon across an alpine/subalpine ecotone, Green Lakes Valley, Colorado Front Range United States. Water Resour. Res. 39, 1188–1200.
Jiao, N., Herndl, G.J., Hansell, D.A., Benner, R., Kattner, G., Wilhelm, S.W., Kirchman, D.L., Weinbauer, M.G., Luo, T., Chen, F., Azam, F., 2010. Microbial production of recalcitrant dissolved organic matter: long-term carbon storage in the global ocean. Nat. Rev. Microbiol. 8, 593–599, http://dx.doi.org/10.1038/nrmicro2386.
Jørgensen, L., Stedmon, C.A., Kragh, T., Markager, S., Middelboe, M., Søndergaard, M., 2011. Global trends in the fluorescence characteristics and distribution of marine dissolved organic matter. Mar. Chem. 126, 139–148.
Kowalczuk, P., Cooper, W.J., Durako, M.J., Kahn, A.E., Gonsior, M., 2009. Characterization of dissolved organic matter fluorescence in the South Atlantic Bight with use of PARAFAC model: interannual variability. Mar. Chem. 113, 182–196.
Kowalczuk, P., Cooper, W.J., Durako, M.J., Kahn, A.E., Gonsior, M., Young, H., 2010. Characterization of dissolved organic matter fluorescence in the South Atlantic Bight with use of PARAFAC model: relationship between fluorescence and its components, absorption coefficients and organic carbon concentration. Mar. Chem. 118, 22–36.
Lawaetz, A.J., Stedmon, C.A., 2009. Fluorescence intensity calibration using the Raman Scatter peak of water. Appl. Spectrosc. 63, 936–940.
Lai, B., Zhou, Y.X., Yang, P., 2013. Treatment of wastewater from acrylonitrile-butadiene-styrene (ABS) resin manufacturing by biological activated carbon (BAC). J. Chem. Technol. Biotechnol. 88, 474–482.
Maie, N., Scully, N.M., Pisani, O., Jaffé, R., 2007. Composition of a protein-like fluorophore of dissolved organic matter in coastal wetland and estuarine ecosystems. Water Res. 41, 563–570.

McKnight, D.M., Boyer, E.W., Westerhoff, P.K., Doran, P.T., Kulbe, T., Andersen, D.T., 2001. Spectrofluorometric characterization of dissolved organic matter for indication of precursor organic material and aromaticity. Limnol. Oceanogr. 46, 38–48.

Murphy, K.R., Stedmon, C.A., Waite, T.D., Ruiz, G., 2008. Distinguishing between terrestrial and autochthonous organic matter sources in marine environments using fluorescence spectroscopy. Mar. Chem. 108, 40–58.

Ohno, T., Bro, R., 2006. Dissolved organic matter characterization using multiway spectral decompostion of fluorescence landscapes. Soil Sci. Soc. Am. J. 70, 2028–2037.

Osburn, C.L., Stedmon, C.A., 2011. Linking the chemical and optical properties of dissolved organic matter in the Baltic-North Sea transition zone to differentiate three allochthonous inputs. Mar. Chem. 126, 281–294.

Parlanti, E., Worz, K., Geoffroy, L., Lamotte, M., 2000. Dissolved organic matter fluorescence spectroscopy as a tool to estimate biological activity in a coastal zone submitted to anthropogenic inputs. Org. Geochem. 31, 1765–1781.

Pautler, B.G., Woods, G.C., Dubnick, A., Simpson, A.J., Sharp, M.J., Fitzsimons, S.J., Simpson, M.J., 2012. Molecular characterization of dissolved organic matter in glacial ice: coupling natural abundance ^{1}H NMR and fluorescence spectroscopy. Environ. Sci. Technol. 46, 3753–3761.

Peiris, R.H., Hallé, C., Budman, H., Moresoli, C., Peldszus, S., Huck, P.M., Legge, R.L., 2010. Identifying fouling events in a membrane-based drinking water treatment process using principal component analysis of fluorescence excitation–emission matrices. Water Res. 44, 185–194.

Peldszus, S., Hallé, C., Peiris, R.H., Hamouda, M., Jin, X., Legge, R.L., Budman, H., Moresoli, C., Huck, P.M., 2011. Reversible and irreversible low-pressure membrane foulants in drinking water treatment: identification by principal component analysis of fluorescence EEM and mitigation by biofiltration pretreatment. Water Res. 45, 5161–5170.

Santos, L.M., Simões, M.L., Melo, W.J., Martin-Neto, L., Pereira-Filho, E.R., 2010. Application of chemometric methods in the evaluation of chemical and spectroscopic data on organic matter from oxisols in sewage sludge applications. Geoderma 155, 121–127.

Senesi, N., D'Orazio, V., Ricca, G., 2003. Humic acids in the first generation of eurosoils. Geoderma 116, 325–344.

Singh, S., D'Sa, E.J., Swenson, E.M., 2010. Chromophoric dissolved organic matter (CDOM) variability in Barataria Basin using excitation–emission matrix (EEM) fluorescence and parallel factor analysis (PARAFAC). Sci. Total Environ. 408, 3211–3222.

Stedmon, C.A., Bro, R., 2008. Characterizing dissolved organic matter fluorescence with parallel factor analysis: a tutorial. Limnol. Oceanogr: Methods 6, 572–579.

Stedmon, C.A., Markager, S., 2005. Resolving the variability in dissolved organic matter fluorescence in a temperate estuary and its catchment using PARAFAC analysis. Limnol. Oceanogr. 50, 686–697.

Stedmon, C.A., Markager, S., Bro, R., 2003. Tracing dissolved organic matter in aquatic environments using a new approach to fluorescence spectroscopy. Mar. Chem. 82, 239–254.

Stedmon, C.A., Thomas, D.N., Granskog, M., Kaartokallio, H., Papadimitriou, S., Kuosa, H., 2007. Characteristics of dissolved organic matter in Baltic coastal sea ice: allochthonous or autochthonous origins? Environ. Sci. Technol. 41, 7273–7279.

Wang, Z., Liu, W., Zhao, N., Li, H., Zhang, Y., Si-Ma, W., Liu, J., 2007. Composition analysis of colored dissolved organic matter in Taihu Lake based on three dimension excitation–emission fluorescence matrix and PARAFAC model, and the potential application in water quality monitoring. J. Environ. Sci. 19, 787–791.

Wei, L.L., Zhao, Q.L., Xue, S., Jia, T., Tang, F., You, P.Y., 2009. Behavior and characteristics of DOM during a laboratory-scale horizontal subsurface flow wetland treatment: effect of DOM derived from leaves and roots. Ecol. Eng. 35, 1405–2141.

Weishaar, J.L., Aiken, G.R., Bergamaschi, B.A., Fram, M.S., Fujii, R., Mopper, K., 2003. Evaluation of specific ultraviolet absorbance as an indicator of the chemical composition and reactivity of dissolved organic carbon. Environ. Sci. Technol. 37, 4702–4708.

Yamashita, Y., Jaffé, R., 2008. Characterizing the interactions between trace metals and dissolved organic matter using excitation–emission matrix and parallel factor analysis. Environ. Sci. Technol. 42, 7374–7379.

Yamashita, Y., Jaffé, R., Maie, N., Tanoue, E., 2008. Assessing the dynamics of dissolved organic matter (DOM) in coastal environments by excitation emission matrix fluorescence and parallel factor analysis (EEM-PARAFAC). Limnol. Oceanogr. 53, 1900–1908.

Yamashita, Y., Maie, N., Briceno, H., Jaffe, R., 2010. Optical characterization of dissolved organic matter in tropical rivers of the Guayana Shield, Venezuela. J. Geophys. Res. Biogeol. 115, G00F10, http://dx.doi.org/10.1029/2009JG000987.

Yao, X., Zhang, Y., Zhu, G., Qin, B., Feng, L., Cai, L., Gao, G., 2011. Resolving the variability of CDOM fluorescence to differentiate the sources and fate of DOM in Lake Taihu and its tributaries. Chemosphere 82, 145–155.

Yu, H., Xi, B., Su, J., Ma, W., Wei, Z., He, X., Guo, X., 2010. Spectroscopic properties of dissolved fulvic acids: an indicator for soil salinization in arid and semiarid regions in china. Soil Sci. 175, 240–245.

Zhang, Y., van Dijk, M.A., Liu, M., Zhu, G., Qin, B., 2009. The contribution of phytoplankton degradation to chromophoric dissolved organic matter (CDOM) in eutrophic shallow lakes: field and experimental evidence. Water Res. 43, 4685–4697.